From the Fabricae of Augustus and the Workshops of Charlemagne: A compositional study of corroded copper-alloy artifacts using hand-held portable XRF

Roxburgh, M.A.

Author: Roxburgh, M.A.
Title: From the Fabricae of Augustus and the Workshops of Charlemagne: A compositional study of corroded copper-alloy artifacts using hand-held portable XRF
Issue Date: 2019-12-03

Chapter 2

A Non-destructive survey of early Roman copper-alloy brooches using portable X-ray Fluorescence Spectrometry

M.A. Roxburgh, S. Heeren, D. J. Huisman, B.J.H. Van Os

Published in: Archaeometry, 2 July 2018, https://doi.org/10.1111/arcm.12414

INTRODUCTION

This paper argues that portable X-ray fluorescence spectrometry (pXRF) is a suitable elemental measurement technique with which to study the production of copper-alloy artefacts. Rather than attempt to match the accuracy and precision of laboratory-based techniques, we deploy pXRF in a survey, or screening mode, arguing that it is more suitable to model the social, chronological and geographical nature of 'metal flows' through the non-destructive study of large groups of artefacts (Needham 1998; Pollard et al. 2015). The primary goal of the present research is to investigate to what extent the analyses of the corrosion layer by pXRF can be used for classifying copper-alloy artefacts. The ability to classify objects by their alloy composition is critical if pXRF is to be a valid technique for this approach.

Our approach is to explore the relationship between the form and bulk alloy composition, both of which are intentional actions determined by human choice: the choice of alloy composition can be guided by such factors as raw material availability, workshop organization, and trade or exchange. Many large collections of copper-alloy artefacts have become available for study since the 1970s when the cost and availability of metal detectors resulted in widespread use by both amateur and professional users. Many thousands of these items, which would otherwise have been lost to modern farming practices or building projects, provide ideal data sets for compositional study. Although much of the material has been recovered without a detailed archaeological context - in contrast to those found in carefully planned site excavations - it does provide an opportunity to study trends in availability and choice of alloys in a typological, geographical and chronological context.

By using a large Roman period pXRF data set, measured from collections in the Nijmegen region of the Netherlands, we explore the effectiveness of the technique by comparing the traditionally held problems associated with pXRF against the requirements needed for more socially orientated research models. Other studies have demonstrated the usefulness of the technique for late Roman and early Medieval copper-alloy objects (Roxburgh and Van Os 2018; Roxburgh et al. 2018).

The traditional challenges facing pXRF

Recent years have seen a significant increase in the use of pXRF devices in archaeological research (Shackley 2010, 17), especially those that are compact enough to be held in the hand. These instruments are typically user friendly and allow for a high throughput of non-destructive analysis. Much criticism has been put forward, however, concerning their reliability when used by operators with inadequate analytical training (e.g. Shackley 2010, 17; Speakman and Shackley

2013). The point, shoot and read nature of these devices means they can be operated with the minimum of training and supervision. This does not mean, however, that interpretation of the results should be undertaken at that same operator level. Archaeological pXRF projects should include researchers who are experienced in both the interpretation of compositional data and the basics of XRF analysis (Shackley 2010, 18) to produce valid and reliable results.

Because of the continuing development and miniaturization of the XRF technique, many portable machines on the market today now have superior detector resolution than laboratory equipment in use a decade ago (Frahm and Doonan 2013, 1080; Speakman and Shackley 2013, 1436). Although higher precision and lower detection limits may be obtained with more standard analytical laboratory techniques (e.g., Lab-XRF, neutron activation analysis (NAA), atomic absorption spectrometry (AAS), scanning electron microscopy (SEM) or inductively coupled plasma (ICP) techniques, which are also improving), the need for artefact damage—by drilling or the removal of corroded surface layers—may be problematic for many objects. The non-destructive nature of the technique therefore makes access to and analyses of artefacts possible which would be inaccessible for damaging techniques (see below).

However, while it has been shown that it is possible to obtain reliable compositional data on corroded, ancient copper-alloy surfaces using XRF (Lutz and Pernika 1996), it is still a surface-measuring technique. Therefore, it becomes necessary to consider any compositional variation present on the surface of artefacts. Variation can be caused by sample inhomogeneity, the effects of corrosion, including surface irregularity and variations in thickness. These parameters affect the outcome of all analytical techniques, but in most cases pXRF optimization of sample measurement conditions due to its nature and restrictions placed on it by artefact owners (e.g. forbidding destructive sample preparation) is minimal or lacking.

Despite these less favourable conditions, a number of archaeological applications of pXRF have since been published that include, for instance, insights into the production organization behind the bronze weapons found with the Terracotta Army in Xi'an, China (Martinón-Torres et al. 2012) as well as later Roman and early Medieval studies by the present authors (Roxburgh and Van Os 2018; Roxburgh et al. 2016b, 2017, 2018). A study of both early and late Roman brooches at Richborough, Kent, by Bayley and Butcher (2004) is particularly useful in its comparison of quantitative and qualitative techniques (XRF versus AAS), showing especially that the assignment of alloy names is comparable, but only when measuring large data sets (Bayley 1992, 301; Bayley and Butcher 2004, 22). Lately, the approach has also been applied in an analysis of the social organization behind the production of late Roman brooches in northern Gaul (van Thienen and Lycke 2017).

The use of pXRF devices in archaeometric research is dependent, therefore, on an appropriate methodological approach. This includes adequate sample preparation and a calibration process relying on internationally recognized standards (Kaiser and Shugar 2012). The usefulness of pXRF devices depends on whether the achievable level of measurement accuracy and precision is enough to address a particular archaeological problem.

In the case of metallic artefacts, the major advantage of pXRF devices is that they can be employed in non-destructive analysis. This is especially true for copper-based artefacts where preservation of the patina, or corrosion layer, is often considered to be of great importance by conservators. Since pXRF allows for safe, non-destructive analyses, much larger numbers of artefacts can be released by museum curators. An additional advantage is that analyses are quick and require short preparation times, which allows for faster analyses of large collections, with the same machine and settings. However, more than for other artefacts, the elemental composition of the corrosion layer from alloys will almost certainly differ from the uncorroded core. This would hinder the use of pXRF analyses in a pure 'provenance'role. But the potential for the technique to group artefacts according to variations in their alloy composition and thus engage with a different set of questions—those relating to human interaction, their deliberate choice of alloying elements, recycling practices, questions that reflect social and economic change over broad chronological and geographical frameworks— is certainly large.

Artefact production and compositional variation

The composition of copper-alloy artefacts is influenced by intentional acts by the craftsmen as they manipulated the alloy in a liquid and a solid state. Studying variation in alloy composition is an avenue of research aimed at a better understanding of the social organization of craft production in past societies. For this, we need to determine and group the compositional variation in the alloys of a considerable number of objects of a uniform typology. Comparing alloy composition with form allows us to try to infer, for example, whether or not objects were produced in large production centres and subsequently distributed. Or, conversely, whether they were more likely produced in widely dispersed local workshops. Other, related, inferences could include whether the raw materials came from several sources or from centralized supply centres (e.g. Ling et al. 2014) or if scarcity of the raw materials induced recycling practices (and if that were the case, to what extent different alloys were sorted before being remelted?).

Even when the raw material sources are unknown, the degree of centralization of raw material procurement can be inferred from the compositional variation in the artefacts. Recent pXRF studies on the copper-alloy weaponry found with the terracotta warriors, Martinón-Torres et al. (2012) attempted to shed a light on production organization and craft specialization employed by ancient craftsmen. The degree of compositional uniformity found in large groups of objects such as these is likely to suggest something further about the organization of labour, transmission of technical knowledge and cross-craft interaction. High degrees of uniformity over a wide geographical area could imply that raw materials were sourced and supplied in a centralized fashion, or that artefacts were mass-produced in a central workshop. In contrast, significant compositional variation may indicate separate production modes, and differences in raw material sourcing including variation due to recycling. Thus, the study of artefact composition can provide useful information when investigating the organization of production, providing the right questions are asked.

Analytical challenges

A reliable level of accuracy and precision has previously been demonstrated using XRF on the corrosion layer on copper alloys (Lutz and Pernika 1996). However, the degradation of copper alloys typically results in the formation of a corrosion layer that may be depleted in copper (decuprification) and, therefore, enriched by the alloying metals, when compared with the intact metal core. Different soil types may also influence the rate at which an object corrodes and, therefore, the type of corrosion, its intensity and the direction in which the changes take place interfere with the determination of an original alloy composition for an artefact. To complicate this issue further, surface concentrations may also vary considerably given the heterogeneous distribution of lead globules within a copper alloy (Smit 2012). In addition, deposition of iron hydroxides or sulphides onto metal objects often occurs in the soil. The effect of such an iron-rich layer is that secondary copper radiation is absorbed, but that higher energy secondary tin X-rays are relatively enhanced.

The reflection depth of X-rays in metals is dependent on the mass attenuation of the material and the incident X-ray energy. In metals, the critical reflection depth, i.e., the depth of analyses is restricted for most elements below 0.1 mm (Gigante et al. 2005). As a result, in the case of metals, XRF devices provide the composition of an object's surface and thus will be influenced by compositional changes caused by corrosion effects (see also Gigante et al. 2005; Orfanou and Rehren 2014).

In the present study, we assessed the challenge presented by these surface variations by comparing XRF analyses on corroded and subsequently cleaned surfaces of a group of Roman brooch fragments. We then test whether the corrosion-induced changes in alloy ratios affect the potential for using the data for studying the human choices involved in production.

MATERIALS AND METHODS

Materials

Non-destructive measurements were taken from 187 identifiable bow brooches from the private collection of Harry Sanders, which was made available for scientific study at the Bureau Archeologie & Monumenten at Nijmegen (Table S1). The objects, which dated between 150BC and 200AD were all recovered during archaeological fieldwork in and around the city of Nijmegen and from metal detection in ploughed fields in neighbouring municipalities. Nijmegen is located on the south bank of the River Waal (a branch of the Rhine) and was the site of a major Roman military and civil centre, situated on a hill at the apex of the Rhine and Meuse delta. The soils around Nijmegen and those to the south are generally sandy, well drained and relatively acidic (podzol types). North of the river, however, the region is dominated by clayey lime-buffered soils with elevated groundwater tables. There were 14 additional bow brooch fragments (reserved for destructive mechanical cleaning) that were recovered from the villages of Elst and Oosterhout, both on the northern side of the river.

The following common typological names have been used to identify the brooch types in this survey. The earliest measured is the pre-Roman Nauheim series (150 to 70BC), included as a comparison for the following early Roman types. For the 187 complete brooches, we have the Aucissa, Eye and Almgren 15 series (20BC– 80AD, 5–100AD and 30–180AD respectively), then the corrosion test includes 14 additional brooch fragments, including fragments from the Almgren 20 series (20BC–100AD) and also van Buchem 24 and Böhme 19 variants (both second century AD). See Heeren and van der Feijst (2017), types 8, 30, 20, 45, 17, 47– 48 and 51 respectively for recent typological analyses and links to earlier publications. A common manufacturing characteristic for brooches of this period was that many types were wrought (hammered) out of a single piece of copper alloy, including the spring (Bayley and Butcher 2004, 32). This meant these particular brooches were made in a extremely low or unleaded alloy, because of the working limitations of lead in alloys (Bayley and Butcher 2004, 15). Other brooch types were composed of multipiece assemblies, with the spring being made separately from the body of the brooch. This meant that higher proportions of lead could be added to the main body because it was made separately from the spring. Of the brooch types used in this study, the Aucissa and Böhme 19 variants are multipiece assemblies. The rest are one-piece variants.

The organization behind brooch production is still attracting archaeological debate. One theory being explored is that brooch production was linked to military workshops, primarily due to their similarity in form to a number of military items (Roxburgh et al. 2016a, 413). The Aucissa type, for example, is considered by some to be the soldiers brooch, which if the case allows the question to be posed as to whether all brooches at this time had a close relation to the army or whether some types were more local in nature, perhaps linked to a particular regional group, which may be the case for the Almgren 15 series (Heeren and van der Feijst 2014, 99). The debate surrounding the introduction of brass into Roman production is of some importance to this question. It is thought that brass was first produced on an industrial scale during the first century BC (Bayley1998, 8–9). Furthermore it is also thought that during this early period the Roman state reserved it for the production of military gear and coins, but at some point towards the end of the first century AD its use rapidly declines (Bayley and Butcher 1995, 118; Dungworth 1997, 903). To engage this debate with pXRF, large numbers of individual brooches from well-defined typologies are required in order to assess how homogeneous they are over a wide area. This cannot as yet be done through other methods requiring the destructive cleaning or sampling of large numbers of items. If pXRF can do this non-destructively, then a comparison can be made between pre-conquest and Roman period production (between brass and bronze use in particular), then further an exploration of alloy types found at later military production sites can be compared with local tribal settlements.

For the Netherlands (the province of Germania Inferior in Roman times) this ability to explore alloy choice and the level of homogeneity present in large numbers of brooch types enables useful comparisons to be drawn with research in other regions, such as that undertaken by Bayley and Butcher (2004) at Richborough in Britain.

Methods

pXRF

A Niton XL3t GOLDD Handheld XRF analyser was used for this study. It was factory calibrated with standards for metals and alloys and equipped with a large area silicon drift detector with optimized geometry. The electronic metals mode was selected and used throughout the data-gathering phase. This takes an off-the-shelf approach rather than rely on the development of custom calibrations. The advantage of this mode is that the same metals of interest (i.e., those found in Roman and Medieval alloys) are used in modern electronic equipment (Cu, Sn, Ag, Zn, Au), or are marked as potential hazardous materials (Pb, Hg, As, Se). In order to test whether this mode, which may not have been originally designed for use on copper alloys, was suitable for this application, we tested its performance on the Cultural Heritage Alloy Reference Material Set (CHARM) set of reference metals (see below).

The analyser was mounted on a portable test bench (hence, we use pXRF not hhXRF; see Frahm and Doonan, 2013, 1426, for further labelling discussion), with a lead cover to provide a consistent operating environment whilst protecting the user from radiation. The test bench made it possible to place the objects over the 8 mm spot size easily. In most cases the objects fully covered the opening, but some were slightly smaller. However, slightly varying the angle of the object to the opening, including the amount of coverage across the opening, was found to be insignificant in terms of the method proposed here. By checking the machine read-out during analyses, it was found that the machine-reported analytical error, for the elements of interest, was <0.2% with reading times >35 s, so this reading time was deemed sufficient for the present study (see below for the performance of the analyses with this reading time on the CHARM set of reference materials). Two spectrum readings per 35 s intervals were taken, the first for the main range of elements at 50 kV (Cu-K to Ba-K, and Au-L to Pb-L) and the second for the low range at 10 kV (Al-K to Cu-K). After the analyses, the spectra were checked individually for inconsistencies and unexpected overlaps. Based on these checks, the analytical values for arsenic were discarded because of a peak overlap of lead.

One measurement was taken for each item, on the front, central bow section of the brooch, or on the front, head or foot sections when fragments were used. An external normalization of the completed data set in a spreadsheet program (Microsoft Excel™) was then undertaken, which corrected for the contribution of the light elements that would be present in the patina due to contamination from soil residues (such as sand, clay and iron hydroxides). The elemental concentrations of the alloying elements were normalized on a light elements (Si-Fe)-free basis. In the present paper, only the main alloying elements (Cu, Sn, Zn, Pb) are considered. The factory calibration of the device was checked against the reference samples of the copper CHARM set (Heginbotham et al. 2015). The results (Table 1 and Fig. 1) show that standard deviations remain within a few per cent. Plotting the results in a ternary diagram, such as the one uses for all analyses results (see below), shows no deviation for all but one of the samples. Only sample 32xLB10 deviates in its lead content, possibly due to the inhomogeneity that is common for leaded copper alloys.

Corrosion study

The study was conducted in a similar manner to that of Fernandes et al. (2013) by comparing the compositions of the corrosion layer and uncorroded core of the artefacts. Contrary to some of the Fernandes et al. objects, we fully removed the corrosion layer for all tested artefacts. The pXRF analyses were conducted on both corroded and cleaned surfaces and typically 0.5–1.0 mm in depth were removed to reach the uncorroded core (Fig. 2, inset), using the same type of Niton machine as described above, including settings and calibration.

Visualization of compositional data

The study of copper alloys in Roman Britain by Bayley and Butcher (1995, 2004) demonstrated the effectiveness of using triangular (ternary) diagrams for visualizing the concentrations of Sn, Zn and Pb measured using AAS (Fig. 2). The study identified multiple distinct compositional groups of Roman brooches that matched well with typo-chronological groupings. The use of ternary diagrams implies that concentrations of the selected alloying elements (Sn, Zn, Pb) are normalized to 100% so that copper content is not taken into account. This has a disadvantage that objects that are almost pure copper without care will still be classified as an alloy (e.g., a bronze or brass) on the basis of very low concentrations of alloying elements. It is important, therefore, that an assessment of the data is made before producing these diagrams—checking and removing items produced in copper, lead or tin, for example. The measurements should also be used as reference when interpreting the nature of any groups present, such as determining if certain elements were deliberately added or not. It must also be kept in mind that the alloy classification in these diagrams does not match the common alloy definitions based on absolute concentrations. A major benefit, however, is that large numbers of compositional analyses can be visualized in one diagram, so that trends in alloy choice can be identified for differing groups of artefacts. Bayley and Butcher (1995, 2004) have set a benchmark by showing how compositional variation—in their case determined by AAS analyses—as depicted in triangular diagrams is especially suitable for Roman fibulae, and how distinct groups are easily distinguished by eye.

Pollard et al. (2015) applied a different approach for interpreting a large database of copper-alloy artefacts: they classified copper alloy artefacts based on absolute concentrations, using a threshold of 1% to identify deliberately added alloying elements to the metal melt. The present approach is different, partly out of necessity: a 1% threshold cannot be maintained in corrosion-affected measurement data. More important, however, is that a 'hard' a priori classification may not do justice to the actual grouping that, for example, become apparent in ternary graphs such as those published by Bayley and Butcher (1995, 2004). Visually assessing the degree of separation between groups, or recognizing mixing lines between end members is a necessity for studying trends in alloy choice that is only possible by using such graphs. Bayley and Butcher (2004, 24) divided their ternary diagrams into alloy classes (Fig. 1, inset). These classes (e.g., brass, bronze and gunmetal) are of course associated with terminology employed in modern metallurgy. A hard classification between leaded and unleaded alloys is also not maintainable in corroded objects so a qualitative judgement based on the construction limitations mentioned above is preferred (i.e., one typological group may systematically show a higher lead measurement than another). In the present diagrams, we indicate a simplified version of this classification (with brass (>4% Zn), bronze (≥3% Sn) as background without imposing a rigid classification. Note that these diagrams do not include copper contents and are therefore not suitable for determining alloy properties.

It is also important to understand that ancient names and their corresponding alloy ratios are not well understood (Bayley and Butcher 2004, 14). Attempts to impose rigid modern classifications would be unlikely to reflect historical boundaries, intentionally created or otherwise, by ancient craftsmen. Plotting large numbers of measurements in ternary diagrams and observing their distributions allows for a better understanding of historical boundaries and, therefore, technical choices. In the present study, we therefore only lightly touch on this classification, and put more confidence in the study of alloy distributions in ternary diagrams.

Pb	Measured values				Reference values		Differences	
	Mean	St. Dev.	RSD(%)	CI (95%)	Mean	CI (95%)	Delta	Delta %
31X 7835.8	2.88	0.031	1.09	0.022	3.2	0.03	0.32	9.9
31X 7835.9	1.15	0.022	1.95	0.012	1	0.017	-0.15	-14.6
31X TB5	0.58	0.014	2.41	0.007	0.6	0.007	0.02	3.2
32X LB10	9.57	0.042	0.43	0.022	11.7	0.07	2.13	18.2
32X LB14	14.92	0.076	0.51	0.044	14.6	0.06	-0.32	-2.2
32XLB17	9.77	0.019	0.20	0.01	9.8	0.1	0.03	0.3
32X SN5	0.32	0.010	3.18	0.005	0.3	0.004	-0.02	-6.4
32X SN6	1.73	0.020	1.18	0.011	1.6	0.015	-0.13	-7.9
32X SN7	2.64	0.028	1.08	0.015	2.6	0.03	-0.04	-1.6
32X GM4	4.91	0.034	0.68	0.018	4.7	0.04	-0.21	-4.5
33X GM20	0.12	0.008	6.57	0.004	0.1	0.002	-0.02	-15.8
33X GM21	6.69	0.032	0.47	0.017	7	0.05	0.31	4.4
Zn								
	Mean	St. Dev.	RSD(%)	CI (95%)	Mean	CI (95%)	Delta (Ref. -	Delta %
31X 7835.8	25.66	0.047	0.18	0.039	24.8	0.06	-0.86	-3.5
31X 7835.9	14.53	0.018	0.13	0.01	14.3	0.06	-0.23	-1.6
31X TB5	41.27	0.050	0.12	0.026	40.6	0.15	-0.67	-1.6
32X LB10	0.56	0.005	0.84	0.003	0.6	0.009	0.04	6.8
32X LB14	0.04	0.005	14.06	0.004	0	0.024	-0.04	-
32XLB17	0.64	0.007	1.10	0.004	0.6	-	-0.04	-6.0
32X SN5	0.49	0.011	2.35	0.006	0.5	0.005	0.01	2.7
32X SN6	1.19	0.013	1.09	0.007	1.2	0.02	0.01	0.9
32X SN7	1.95	0.010	0.51	0.005	2	0.02	0.05	2.5
32X GM4	7.21	0.023	0.31	0.012	7.1	0.04	-0.11	-1.6
33X GM20	3.91	0.016	0.40	0.008	3.9	0.04	-0.01	-0.1
33X GM21	5.28	0.013	0.25	0.007	5.1	0.04	-0.18	-3.5
Sn								
	Mean	St. Dev.	RSD(%)	CI (95%)	Mean	CI (95%)	Delta (Ref. -	Delta %
31X 7835.8	0.48	0.0036012	0.74	0.003	0.5	0.007	0.02	3.0
31X 7835.9	1.53	0.0125432	0.82	0.007	1.5	0.02	-0.03	-2.2
31X TB5	0.11	0.0026662	2.42	0.001	0.1	0.003	-0.01	-10.2
32X LB10	8.14	0.0153391	0.19	0.008	8.2	0.09	0.06	0.8
32X LB14	5.30	0.0200469	0.38	0.011	5.4	0.034	0.10	1.9
32XLB17	5.92	0.0142643	0.24	0.008	6	0.04	0.08	1.3
32X SN5	16.94	0.048693	0.29	0.026	16.1	0.09	-0.84	-5.2
32X SN6	7.55	0.0182118	0.24	0.01	7.3	0.03	-0.25	-3.5
32X SN7	12.84	0.0212551	0.17	0.011	12.6	0.09	-0.24	-1.9
32X GM4	2.55	0.0071798	0.28	0.004	2.6	0.05	0.05	1.9
33X GM20	4.25	0.0093724	0.22	0.005	4.1	0.02	-0.15	-3.7
33X GM21	4.48	0.0189098	0.42	0.01	4.6	0.03	0.12	2.5

Table 1 Results of the measurements from the Cultural Heritage Alloy Reference Material Set (CHARM) reference set for lead (Pb), zinc (Zn) and tin (Sn) compared with the reference values and 95% confidence interval (CI) range

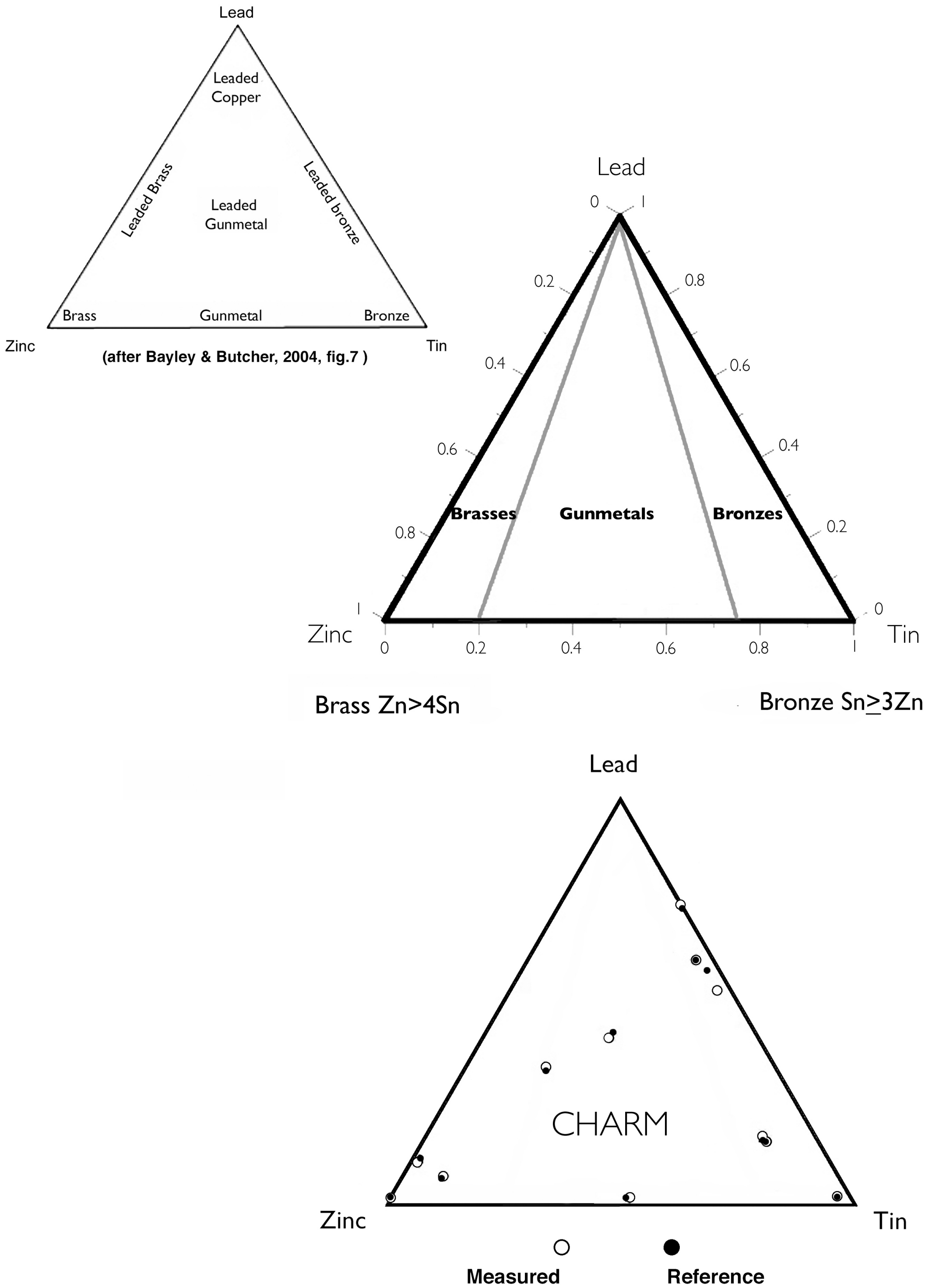

Figure 1 Ternary graphs (after Bayley and Butcher 2004, fig. 7): (upper and middle graphs) simplified classifications; and (lower graph) measured and reference values from the Cultural Heritage Alloy Reference Material Set (CHARM) reference alloy set. Note the deviation of one sample (32X LB10). This sample has a systematic lower measured lead content.

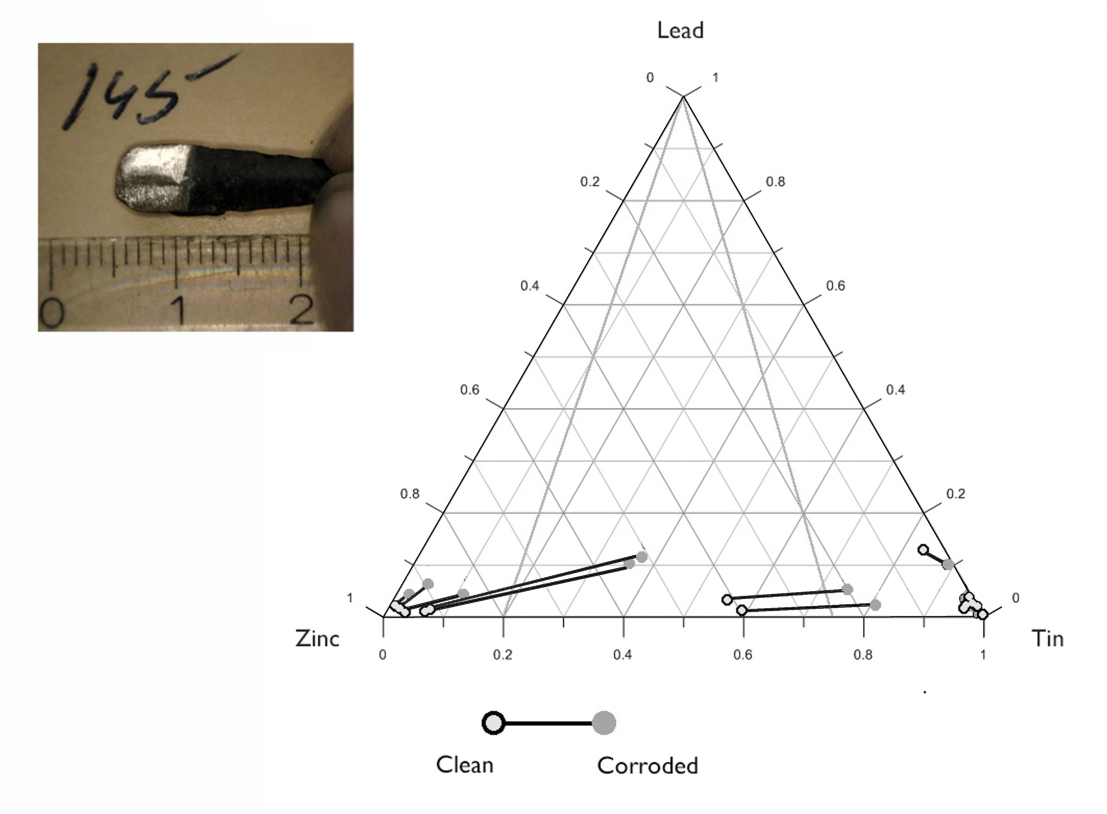

Figure 2 Comparison of measurements made on the corrosion layers and cleaned metal. Black lines connect measurements to the same object.

RESULTS

Corrosion effects on pXRF analyses

A comparison of the corroded and uncorroded measurements on the Nijmegen brooch fragments is shown in Table 2 (for additional data, see Table S1). In general, we can see an average depletion in copper contents of 35% for the seven brooches alloyed with tin. For the two brooches having relatively high tin and zinc contents, the average depletion in copper was 18.5%, but only a small depletion of 0.7% zinc was observed. The remaining five brooches were alloyed with zinc and exhibited a zinc depletion of 9%.

The results show that decuprification and dezincification represented the main corrosion processes at work. Depletion in copper content was observed to be the most relevant change in bronzes and the leaching of zinc from brass objects was also common.

When plotted in a ternary diagram, the effects of corrosion and heterogeneity can be compared with the alloy groups (Fig. 2). Since a triangular diagram is based on a copper-free recalculation (so Sn + Pb + Zn = 100%), small variations of alloying elements in copper-rich alloys are magnified. The comparison shows that two measurements that initially are classified as bronze after cleaning become gunmetal. A further two measurements that initially fall into the gunmetal classification with around 50% zinc after cleaning cross into the brass classification, with a new value of 95% zinc—although the composition has not changed. There is also a leaded bronze measurement that also sees a slight increase in lead and an associated decrease in tin. This may be due to the inhomogeneous distribution of lead in copper alloys. For the remaining nine items, the corrosion effects are limited in the sense that they still fall within the same broad compositional group. For our study, it is important to realize that the corrosion effects have not affected the overall grouping; the zinc-dominated alloys ('brass'), the tin-dominated alloys ('bronze') and the intermediate ones ('gunmetal') are still recognizable as distinct clusters, even though the 'brass' group shows more inter-artefact variation, especially those samples with a high copper (i.e., low alloying elements) content.

Grouping the early Roman brooches

The Nauheim brooches appear to have only been made with tin, whereas the (later) Aucissa brooches are made with zinc (Fig. 3) (for the data set for the Nijmegen brooches, see also Table S1). This observation is in line with the brass alloys from Roman period brooches and military equipment found in Masada, Israel, as well as in Britain and other locations in Western Europe (Bishop and Coulston 1993; Ponting and Segal 1998; Bayley and Butcher 2004) The group of measurements for the Eye brooch series show that they are also zinc based, similar to the Aucissa brooches. In contrast, however, the measurements for the Almgren 15 wire brooch series reveal two clusters: one tin based, the other showing a mixing line from zinc- to a lead- and tin-based copper alloy. Comparing this with the Eye brooch and the Almgren 15 measurements from Britain (for the British results, see Fig. 3) shows a similar division in zinc- and tin-based series reveal two clusters: one tin based, the other showing a mixing line from zinc- to a lead- and tin-based copper alloy. Comparing this with the Eye brooch and the Almgren 15 measurements from Britain (for the British results, see Fig. 3) shows a similar division in zinc- and tin-based alloys, but with a different distribution for the outliers—probably due to the corrosion processes.

If these distributions are compared with the displacement values seen in Figure 2, the outliers on the Nijmegen results would be more in line with the British results, after decuprification, dezincification or secondary copper X-ray absorption processes have been considered. Although outliers exist in all cases, it is possible to distinguish the core alloy properties when observed in large numbers. Also knowing that the one-piece brooches contain by necessity little or no lead (see the second section), the large proportion of measurements are below the 20% lead line in the ternary graphs.

Group	Find ID	Cu	Sn	Pb	Zn	Ag	Fe
Measurement before cleaning							
Tin-dominant							
	EM-142	35.26	49.81	5.67	0.57	0.17	7.52
	EM-95	43.77	27.06	0.12	0.20	0.13	25.77
	EM-16	55.22	36.50	1.33	0.51	0.11	5.63
	EM-18b	41.89	44.75	1.79	0.45	0.30	9.23
	EM-140	21.15	59.54	0.30	0.17	0.09	17.32
	EM-552	78.57	20.10	0.45	0.18	0.07	0.31
	EM-597	71.87	25.44	0.56	0.56	0.09	1.02
Gun metal-like							
	EM-902	69.25	17.80	1.26	4.81	0.15	6.02
	EM-655	63.59	24.88	0.72	5.20	0.13	4.69
Zinc-dominated							
	EM-007	85.95	0.27	0.55	11.87	0.03	1.10
	EM-492	85.02	0.53	0.80	11.16	0.07	1.85
	EM-540	81.75	1.28	0.50	9.62	0.07	5.55
	OH-145	79.65	5.86	1.81	8.07	0.08	3.68
	EM-018a	78.81	5.78	1.69	8.74	0.12	4.12
Measurement after cleaning							
Tin-dominant							
	EM-142	83.36	13.44	2.07	0.66	0.07	0.20
	EM-95	85.43	13.65	0.05	0.07	0.10	0.42
	EM-16	85.90	12.98	0.29	0.31	0.05	0.27
	EM-18b	87.66	10.91	0.40	0.13	0.12	0.39
	EM-140	81.37	17.77	0.05	0.09	0.05	0.48
	EM-552	86.04	13.36	0.25	0.08	0.05	0.11
	EM-597	83.78	14.84	0.23	0.45	0.08	0.32
Gun metal-like							
	EM-902	85.04	7.55	0.42	5.65	0.10	0.92
	EM-655	84.82	8.50	0.17	5.79	0.07	0.44
Zinc-dominated							
	EM-007	80.74	0.17	0.35	17.99	0.04	0.64
	EM-492	79.29	0.29	0.36	19.54	0.02	0.43
	EM-540	80.77	0.57	0.11	17.92	0.03	0.39
	OH-145	77.99	1.34	0.19	20.15	0.05	0.19
	EM-018a	79.01	1.35	0.27	18.97	0.04	0.23
Absolute differences							
Tin-dominant							
	EM-142	48.10	-36.36	-3.60	0.09	-0.10	-7.32
	EM-95	41.66	-13.41	-0.07	-0.13	-0.03	-25.35
	EM-16	30.68	-23.52	-1.04	-0.20	-0.06	-5.35
	EM-18b	45.78	-33.84	-1.40	-0.33	-0.18	-8.84
	EM-140	60.22	-41.77	-0.25	-0.08	-0.03	-16.84
	EM-552	7.47	-6.74	-0.20	-0.10	-0.03	-0.20
	EM-597	11.91	-10.61	-0.33	-0.11	-0.01	-0.70
Gun metal-like							
	EM-902	15.79	-10.26	-0.84	0.84	-0.05	-5.10
	EM-655	21.23	-16.39	-0.56	0.59	-0.06	-4.25
Zinc-dominated							
	EM-007	-5.21	-0.10	-0.20	6.11	0.01	-0.46
	EM-492	-5.74	-0.25	-0.44	8.38	-0.05	-1.42
	EM-540	-0.99	-0.71	-0.39	8.30	-0.05	-5.15
	OH-145	-1.66	-4.53	-1.63	12.08	-0.03	-3.49
	EM-018a	0.20	-4.44	-1.42	10.22	-0.08	-3.89

Table 2 Comparison of corroded versus cleaned measurements

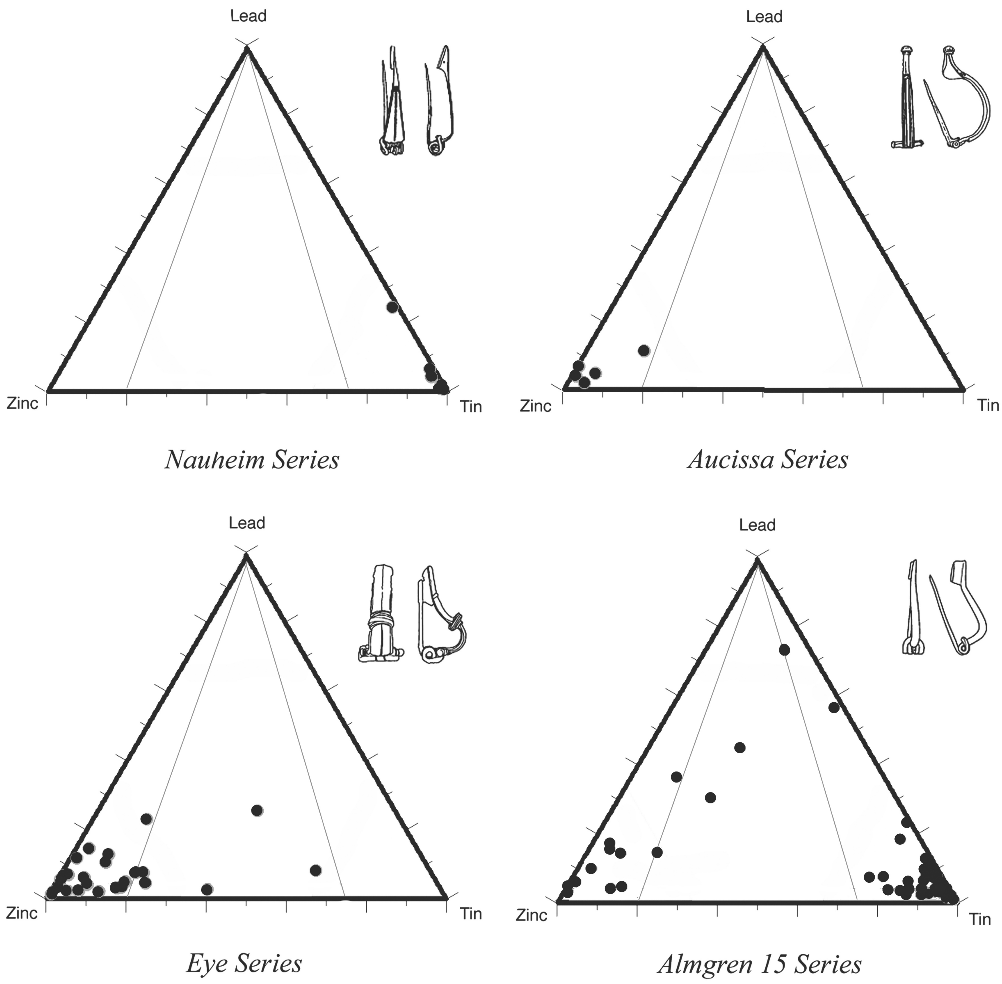

Comparative British Results

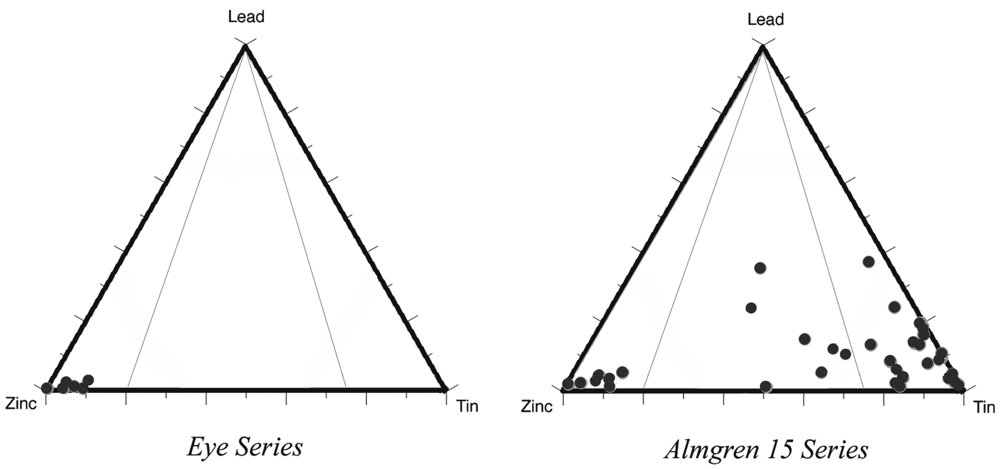

Figure 3 Nijmegen portable X-ray fluorescence spectrometry (pXRF) results versus Bayley and Butcher’s atomic absorption spectrometry (AAS) results (after Bayley and Butcher 1995,figs 3 and 4.1)

DISCUSSION

The tests on the CHARM reference set showed good levels of accuracy and precision under more ideal analytical circumstances. On corroded brooches, however, lack of sample preparation and non-ideal measurement conditions (e.g., not removing the corrosion layer, or preparing a flat surface and variations in angle of brooch to sensor), do not prevent a broader classification of alloys into zinc- or tin-rich traditions. Within the limitations of this measurement method (e.g., no removal of the corrosion layer) we can still address relevant archaeological questions such as those mentioned above.

The offsets between corroded and uncorroded compositions demonstrated that the corrosion effects do not preclude the recognition of separate alloy groups. A measurement taken from a corroded item subsequently classified, for example, as zinc based will not have come from a tin-based alloy.

The results for the Nijmegen study can therefore be compared with the trends found by Bayley and Butcher (1995, 2004). Although we measured the corrosion layer, it is clear that pXRF measurements on corroded brooches can be classified broadly into archaeologically relevant groups.Therefore, subsequent interpretations can be formed alongside those presented in more ideal circumstances. Furthermore, because the rapid and non-destructive technique allows for more items to be measured than with any other method (enabling the better definition of the core distribution for brooch types), it gives a better chronological resolution, allowing a closer view of the transition between types such as those objects changing from bronze to brass, or those staying in bronze during the early Roman period.

CONCLUSIONS

Systematic compositional differences for the major elements (tin, lead, zinc) are observed between the corroded surfaces and the uncorroded metal cores. However, the magnitude of these changes only becomes relevant when considering the specific research question. For questions needing simple alloy classification, achieved through identifying the compositions of large sets of artefacts, it has been shown that compositional ratios remain within a satisfactory tolerance. The results for Nijmegen showed a difference between pre-Roman and early Roman brooches, the former being produced in a tin-rich tradition and the latter in a zinc tradition. Furthermore, where two alloy traditions were present within a brooch series, it was noticed that the same was true of the same series measured in Britain.

It has been demonstrated, therefore, that data provided by an appropriate application of pXRF—perhaps best described as a survey or reconnaissance role—are reliable enough to detect the deliberate control of composition between typological, copper-alloy groups and that the data are comparable with earlier research.

Understanding more about how corrosion affects the results of non-destructive measurements is an important step forward in adopting an appropriate application of pXRF to archaeological copper alloy. Once an association between typology and alloy is identified using this approach, the next step would be to explore the results in more detail using much fewer, carefully selected examples under more rigorous laboratory conditions.

REFERENCES

Bayley, J., 1992. *Non-ferrous metalworking in England: Late Iron Age to early Medieval.* Unpublished Ph.D. thesis, University of London.

Bayley, J., 1998. The production of brass in antiquity with particular reference to Roman Britain. In: P. T. Craddock (ed), *2000 Years of zinc and brass*, Occasional Paper No. 50, revised edition, London: British Museum Press, 7-26.

Bayley, J. and S. Butcher, 1995. The composition of Roman brooches found in Britain. In: S. T. A. M. Mols. (ed), *Acta of the 12th International Congress on Ancient Bronzes, Nijmegen 1992*. Nijmegen: Provincial Museum G. M. Kam, 113-119.

Bayley, J. and S. Butcher, 2004. *Roman brooches in Britain: A technological and typological study based on the Richborough collection*. London: Society of Antiquaries

Bishop, M. C. and J.C.N. Coulston, 1993. *Roman military equipment*. London: Batsford.

Dungworth, D., 1997. Roman copper-alloys: analysis of artefacts from Northern Britain. *Journal of Archaeological Science* 24, 901–910.

Fernandes, R. and B.J.H. van Os and D.J. Huisman, 2013. The use of hand-held XRF for investigating the composition and corrosion of Roman copper-alloyed artefacts. *Heritage Science* 1, 30.

Frahm, E. and R.C.P. Doonan, 2013. The technological versus methodological revolution of portable XRF in archaeology. *Journal of Archaeological Science* 40, 1425–1434.

Gigante, G. E. and P. Ricciardi and S. Ridülfi, 2005. Areas and limits of employment of portable EDXRF equipment for in situ investigations. *ArchéoSciences, Revue d'Archéométrie* 29, 51–59.

Heeren, S. and L. van der Feijst, 2014. De fibulae van de Late Ijzertijd tot de Ottoonse tijd, in Odyssee op het Kops Plateau 2. In: H. van Enckevort (ed), *Aardewerk en fibulae uit Nijmegen-Oost*, ABNij Report No. 47, Nijmegen: Bureau Archeologie Monumenten gemeente Nijmegen, 81-120.

Heeren, S., and L. van der Feijst, (eds), 2017. *Prehistorische, Romeinse en middeleeuwse fibulae uit de Lage Landen. Beschrijving, analyse en interpretatie van een archeologische vondstcategorie*, Amersfoort: Private Press.

Heginbotham, A., J. Bassett, D., Bourgarit, C. Eveleigh, L. Glinsman, D. Hook, D. Smith, R. J. Speakman, A. Shugar and R. Van Langh, 2015. The copper CHARM set: a new set of certified reference materials for the standardization of quantitative X-ray fluorescence analysis of heritage copper alloys, *Archaeometry* 57(5), 856–868.

Kaiser, B. and A. Shugar, 2012. Glass analysis utilizing handheld X-ray fluorescence. In: A. N. Shugar and J. L. Mass (eds), Handheld XRF for art and archaeology, *Studies in Archaeological Sciences*, Leuven: Leuven University Press, 449-470.

Ling, J., Z. Stos-Gale, L. Grandin, K. Billström, E. Hjärthner-Holdar and P.-O. Persson, 2014. Moving metals II: Provenancing Scandinavian Bronze Age artefacts by lead isotope and elemental analyses, *Journal of Archaeological Science* 41, 106–132.

Lutz, J. and E. Pernicka, 1996. Energy dispersive X-ray fluorescence analysis of ancient copper alloys: empirical values for precision and accuracy, *Archaeometry* 38 (2), 313–323.

Martinón-Torres, M., X.J. Lee, A. Brevan, Y. Xia, K. Zhao and T. Rehren, T., 2012. Forty thousand arms for a single emperor: from chemical data to the labor organization behind the bronze arrows of the Terracotta Army, *Journal of Archaeological Method and Theory* 21(3), 534–562.

Needham, S. P., 1998. Modelling the flow of metal in the Bronze Age. In: C. Mordant, M. Pernot and V. Rychner (eds) *L'atelier du bronzier en Europe du XX^e^ au VIII^e^ siècle avant notre ère,* vol. 3: Production, circulation et consommation du bronze, Paris: Comite des Travaux Historiques et Scientifiques, 285-307.

Orfanou, V. and T. Rehren, 2014. A (not so) dangerous method: pXRF vs. EPMA-WDS analyses of copper-based artefacts, *Archaeological and Anthropological Sciences* 7(3), 387-397.

Pollard, A. M., P. Bray, C. Gosden, A. Wilson and H. Hamerow, 2015. Characterising copper-based metals in Britain in the first millennium AD: a preliminary quantification of metal flow and recycling, *Antiquity* 89, 697–713.

Ponting, M. and I. Segal, 1998. Inductively coupled plasma atomic emission spectroscopy analyses of Roman military copper-alloy artefacts from the excavations at Masada, Israel, *Archaeometry* 40(1), 109–122.

Roxburgh, M. A., S. Heeren, D. J. Huisman and B. J. H. van Os, 2016a. Early Roman copper-alloy brooch production: a compositional analysis of 400 brooches from Germania Inferior, *Journal of Roman Archaeology* 29, 411–421.

Roxburgh, M., S. Heeren, H. Huisman, and B. van Os, 2017. De koperlegeringen van Romeinsefibulae en hunbetekenis. In S. Heeren and L. van der Feijst (eds) *Prehistorische, Romeinse enm iddeleeuwse fibulae uit de Lage Landen. Beschrijving, analyse en interpretatie van een archeologische vondstcategorie*, Amersfoort: Private Press, 243–258.

Roxburgh, M. A., D. J. Huisman, and B. J .H. van Os, 2016b. The cross and the crucible: the production of Carolingian disc brooches as objects of religious exchange? *Medieval and Modern Matters* 5, 117–132.

Roxburgh, M. A., N. L. IJssennagger, D. J. Huisman, and B. J. H. van Os, 2018. Where worlds collide: a typological and compositional analysis of the copper-alloy mounts from Viking age Walcheren, *The Medieval Low Countries* 5, (in press November 2018).

Roxburgh, M. A., B. J. H. van Os, 2018. A Comparative Compositional Study of 7th- to 11th-century Copper-Alloy Pins from Sedgeford, England and Domburg, the Netherlands, *Journal Medieval Archaeology* 62, issue 2 (in press October 2018).

Shackley, S., 2010. Is there reliability and validity in portable X-ray fluorescence spectrometry (PXRF)? *SAA Archaeological Record* 10, 17–20.

Smit, D., 2012. Handheld X-ray fluorescence analysis of Renaissance bronzes: practical approaches to quantification and acquisition. In: A. N. Shugar and J. L. Mass (eds) *Handheld XRF for Art and Archaeology*, Studies in Archaeological Sciences, Leuven: Leuven University Press, 37-74.

Speakman, R. J. and S. Shackley, 2013. Silo science and portable XRF in archaeology: a response to Frahm, *Journal of Archaeological Science* 40, 1435–1443.

van Thienen, V. and S. Lycke, 2017. From commodity to singularity: the production of crossbow brooches and the rise of the late Roman military elite, *Journal of Archaeological Science* 82, 50–61.

SUPPORTING INFORMATION

Table S1. Nijmegen worksheet and corrosion experiment worksheet

Nijmegen worksheet - part 1 typological data

Collection / Location	**Find ID**	**Description**	**Period**	**XRF No.**
HS Linden	9 w	Bow - Nauheim type	Pre-Roman	98097
HS Linden	9 aw	Bow - Nauheim type	Pre-Roman	98110
HS Linden	9 m	Bow - Nauheim type	Pre-Roman	98113
HS Linden	9 ay	Bow - Nauheim type	Pre-Roman	98116
HS Eimeren	2 413	Bow - Nauheim type	Pre-Roman	5511
HS Eimeren	2 62	Bow - Nauheim type	Pre-Roman	5514
HS Linden	9 179	Bow - Nauheim type	Pre-Roman	5582
HS Elst	EM-061	Bow - Almgren 15	Roman	102850
HS Elst	EM-062	Bow - Almgren 15	Roman	102851
HS Elst	EM-004	Bow - Almgren 15	Roman	102855
HS Elst	EM-068	Bow - Almgren 15	Roman	102856
HS Elst	EM-017	Bow - Almgren 15	Roman	102857
HS Elst	EM-082	Bow - Almgren 15	Roman	102860
HS Elst	EM-058	Bow - Almgren 15	Roman	102861
HS Elst	EM-086	Bow - Almgren 15	Roman	102862
HS Elst	EM-063	Bow - Almgren 15	Roman	102863
HS Elst	EM-085	Bow - Almgren 15	Roman	102864
HS Elst	EM-066	Bow - Almgren 15	Roman	102866
HS Elst	EM-065	Bow - Almgren 15	Roman	102867
HS Elst	EM-0868	Bow - Almgren 15	Roman	102870
HS Elst	EM-059	Bow - Almgren 15	Roman	102875
HS Elst	EM-098	Bow - Almgren 15	Roman	102876
HS Elst	EM-084	Bow - Almgren 15	Roman	102877
HS Elst	EM-099	Bow - Almgren 15	Roman	102881
HS Elst	EM-069	Bow - Almgren 15	Roman	102886
HS Elst	EM-071	Bow - Almgren 15	Roman	102890
HS Elst	EM-080	Bow - Almgren 15	Roman	102892
HS Elst	EM-091	Bow - Almgren 15	Roman	102894
HS Elst	EM-088	Bow - Almgren 15	Roman	102895
HS Elst	EM-064	Bow - Almgren 15	Roman	102897
HS Elst	EM-119	Bow - Almgren 15	Roman	103199
HS Elst	EM-103	Bow - Almgren 15	Roman	103201
HS Elst	EM-108	Bow - Almgren 15	Roman	103205
HS Elst	EM-109	Bow - Almgren 15	Roman	103211
HS Elst	EM-125	Bow - Almgren 15	Roman	103216
HS Elst	EM-111	Bow - Almgren 15	Roman	103219
HS Elst	EM-128	Bow - Almgren 15	Roman	103222

HS Oosterhout	OA-047	Bow - Almgren 15	Roman	103261
HS Oosterhout	OA-114	Bow - Almgren 15	Roman	103267
HS Elst	ELa-10	Bow - Almgren 15	Roman	103294
HS Valburg	VT-10	Bow - Almgren 15	Roman	103295
HS Valburg	VT-01	Bow - Almgren 15	Roman	103303
HS Elst	EAH-050	Bow - Almgren 15	Roman	103322
HS Elst	EM-159	Bow - Almgren 15	Roman	103351
HS Linden	9 309	Bow - Almgren 15	Roman	98005
HS Linden	9 f	Bow - Almgren 15	Roman	98019
HS Linden	9 77	Bow - Almgren 15	Roman	98031
HS Linden	9 100	Bow - Almgren 15	Roman	98036
HS Linden	9 234	Bow - Almgren 15	Roman	98046
HS Linden	9 217	Bow - Almgren 15	Roman	98050
HS Linden	9 138	Bow - Almgren 15	Roman	98056
HS Linden	9 235	Bow - Almgren 15	Roman	98060
HS Linden	9 220	Bow - Almgren 15	Roman	98064
HS Linden	9 181	Bow - Almgren 15	Roman	98067
HS Linden	9 104	Bow - Almgren 15	Roman	98068
HS Linden	9 102	Bow - Almgren 15	Roman	98070
HS Linden	9 ae	Bow - Almgren 15	Roman	98078
HS Linden	9 j	Bow - Almgren 15	Roman	98084
HS Linden	9 g	Bow - Almgren 15	Roman	98090
HS Linden	9 k	Bow - Almgren 15	Roman	98091
HS Linden	9 ai	Bow - Almgren 15	Roman	98105
HS Linden	9 q	Bow - Almgren 15	Roman	98106
HS Linden	9 u	Bow - Almgren 15	Roman	98111
HS Linden	9 bb	Bow - Almgren 15	Roman	98122
HS Raayen	5 u	Bow - Almgren 15	Roman	98142
HS Raayen	5 60	Bow - Almgren 15	Roman	98153
HS Raayen	5 w	Bow - Almgren 15	Roman	98157
HS Raayen	5 m	Bow - Almgren 15	Roman	98169
HS Raayen	5 n	Bow - Almgren 15	Roman	98170
HS Raayen	5 l	Bow - Almgren 15	Roman	98171
HS Raayen	5 k	Bow - Almgren 15	Roman	98172
HS Raayen	5 84	Bow - Almgren 15	Roman	98174
HS Raayen	5 f	Bow - Almgren 15	Roman	98175
HS Raayen	5 b	Bow - Almgren 15	Roman	98181
HS Eimeren	2 308	Bow - Almgren 15	Roman	5367
HS Eimeren	2 a	Bow - Almgren 15	Roman	5394
HS Eimeren	2 c	Bow - Almgren 15	Roman	5401
HS Eimeren	2 n	Bow - Almgren 15	Roman	5404
HS Eimeren	2 l 2013	Bow - Almgren 15	Roman	5415
HS Eimeren	2 f 2013	Bow - Almgren 15	Roman	5420
HS Eimeren	2 3	Bow - Almgren 15	Roman	5463
HS Eimeren	2 g	Bow - Almgren 15	Roman	5472
HS Eimeren	2 d 2012	Bow - Almgren 15	Roman	5474

HS Eimeren	2 e	Bow - Almgren 15	Roman	5476
HS Eimeren	2 500	Bow - Almgren 15	Roman	5493
HS Eimeren	2 728	Bow - Almgren 15	Roman	5518
HS Eimeren	2 732	Bow - Almgren 15	Roman	5520
HS Reeth	11 40	Bow - Almgren 15	Roman	5524
HS Reeth	11 55	Bow - Almgren 15	Roman	5527
HS Reeth	11 123	Bow - Almgren 15	Roman	5528
HS Reeth	11 194	Bow - Almgren 15	Roman	5537
HS Reeth	11 196	Bow - Almgren 15	Roman	5538
HS Reeth	11 177	Bow - Almgren 15	Roman	5546
HS Reeth	11 10	Bow - Almgren 15	Roman	5554
HS Reeth	11 132	Bow - Almgren 15	Roman	5558
HS Linden	9 356	Bow - Almgren 15	Roman	5575
HS Linden	9 194	Bow - Almgren 15	Roman	5576
HS Linden	9 370	Bow - Almgren 15	Roman	5580
HS Linden	9 176	Bow - Almgren 15	Roman	5586
HS Linden	9 406	Bow - Almgren 15	Roman	5587
HS Linden	9 176	Bow - Almgren 15	Roman	5588
HS Linden	9 454	Bow - Almgren 15	Roman	5593
HS Linden	9 297	Bow - Almgren 15	Roman	5598
HS Linden	9 331	Bow - Almgren 15	Roman	5599
HS Linden	9 314	Bow - Almgren 15	Roman	5605
HS Linden	9 387	Bow - Almgren 15	Roman	5607
HS Linden	9 338	Bow - Almgren 15	Roman	5608
HS Linden	9 212	Bow - Almgren 15 related	Roman	98058
HS Linden	9 6	Bow - Almgren 15 related	Roman	98104
HS Linden	9 av	Bow - Almgren 15 related	Roman	98109
HS Eimeren	2 j 2013	Bow - Almgren 15 related	Roman	5407
HS Eimeren	2 s 2013	Bow - Almgren 15 related	Roman	5414
HS Eimeren	2 375	Bow - Almgren 15 related	Roman	5507
HS Eimeren	2 66	Bow - Almgren 15 related	Roman	5519
HS Linden	9 323	Bow - Almgren 15 related	Roman	5609
HS Elst	EM-090	Bow - Almgren 15 related	Roman	102901
HS Elst	EM-070	Bow - Almgren 15 related	Roman	102874
HS Elst	EM-509	Bow - Almgren 15 related	Roman	103350
HS Oosterhout	OA-505	Bow - Almgren 15 related	Roman	103272
HS Linden	9 245	Bow - Almgren 15 related (moulded shoulder)	Roman	98053
HS Linden	9 133	Bow - Almgren 15 related (moulded shoulder)	Roman	98055
HS Linden	9 109	Bow - Almgren 15 related (moulded shoulder)	Roman	98069
HS Raayen	5 j	Bow - Almgren 15 related (moulded shoulder)	Roman	98156
HS Eimeren	2 229	Bow - Almgren 15 related (moulded shoulder)	Roman	5470
HS Eimeren	2 547	Bow - Almgren 15 related (moulded shoulder)	Roman	5496
HS Reeth	11 50	Bow - Almgren 15 related (moulded shoulder)	Roman	5525
HS Reeth	11 57	Bow - Almgren 15 related (moulded shoulder)	Roman	5548
HS Reeth	11 158	Bow - Almgren 15 related (moulded shoulder)	Roman	5560
HS Elst	EM-074	Bow - Almgren 15 related (moulded shoulder)	Roman	102865

HS Oosterhout	OA-079	Bow - Almgren 15 related (moulded shoulder)	Roman	103258
HS Linden	9 347	Bow - Eye series	Roman	98004
HS Linden	9 417	Bow - Eye series	Roman	98006
HS Linden	9 51	Bow - Eye series	Roman	98021
HS Linden	9 d	Bow - Eye series	Roman	98080
HS Linden	9 aj	Bow - Eye series	Roman	98096
HS Linden	9 v	Bow - Eye series	Roman	98098
HS Linden	9 af	Bow - Eye series	Roman	98119
HS Linden	9 ba	Bow - Eye series	Roman	98132
HS Raayen	5 3	Bow - Eye series	Roman	98155
HS Raayen	5 32	Bow - Eye series	Roman	98182
HS Eimeren	2 r	Bow - Eye series	Roman	5382
HS Eimeren	2 g	Bow - Eye series	Roman	5395
HS Eimeren	2 q	Bow - Eye series	Roman	5397
HS Eimeren	2 i 2013	Bow - Eye series	Roman	5421
HS Eimeren	2 e 2013	Bow - Eye series	Roman	5424
HS Eimeren	2 292	Bow - Eye series	Roman	5442
HS Eimeren	2 39	Bow - Eye series	Roman	5443
HS Eimeren	2 46	Bow - Eye series	Roman	5447
HS Eimeren	2 199	Bow - Eye series	Roman	5461
HS Eimeren	2 115	Bow - Eye series	Roman	5471
HS Eimeren	2 f	Bow - Eye series	Roman	5473
HS Eimeren	2 743	Bow - Eye series	Roman	5487
HS Reeth	11 180	Bow - Eye series	Roman	5544
HS Reeth	11 175	Bow - Eye series	Roman	5553
HS Linden	9 295	Bow - Eye series	Roman	5578
HS Linden	9 449	Bow - Eye series	Roman	5602
HS Linden	9 448	Bow - Eye series	Roman	5606
HS Elst	EM-138	Bow - Eye series	Roman	103197
HS Elst	EM-122	Bow - Eye series	Roman	103202
HS Elst	EAH-078	Bow - Eye series	Roman	103360
HS Elst	EG-83	Bow - Eye series	Roman	103343
HS Elst	ELa-08	Bow - Eye series	Roman	103292
HS Arnhem	AS-12	Bow - Eye series	Roman	103280
HS Oosterhout	OA-030	Bow - Eye series	Roman	103260
HS Oosterhout	OA-072	Bow - Eye series	Roman	103259
HS Elst	EM-137	Bow - Eye series	Roman	103221
HS Elst	EM-131	Bow - Eye series	Roman	103207
HS Elst	EG-27	Bow - Eye series, foot, frag	Roman	103341
HS Eimeren	2 740	Bow - Eye series, foot, frag	Roman	5501
HS Eimeren	2 b 2013	Bow - Eye series, foot, frag	Roman	5426
HS Raayen	5 62	Bow - Eye series, foot, frag	Roman	98194
HS Raayen	5 s	Bow - Eye series, foot, frag	Roman	98144
HS Linden	9 190	Bow - Eye series, foot, frag	Roman	98054
HS Linden	9 344	Bow - Aucissa series	Roman	98047
HS Linden	9 ad	Bow - Aucissa series	Roman	98079

HS Linden	9 c 2013	Bow - Aucissa series	Roman	98139
HS Eimeren	2 171	Bow - Aucissa series	Roman	5455
HS Eimeren	2 100	Bow - Aucissa series	Roman	5503
HS Elst	EAH-083	Bow - Aucissa series	Roman	103320
HS Elst	EAH-124	Bow - Aucissa series	Roman	103319
HS Elst	EAH-074	Bow - Aucissa series	Roman	103316
HS Arnhem	AS-16	Bow - Aucissa series	Roman	103282
HS Oosterhout	OA-062	Bow - Aucissa series	Roman	103269
HS Oosterhout	OA-057	Bow - Aucissa series	Roman	103268
HS Eimeren	2 f	Bow - Aucissa series, Alesia	Roman	5396
HS Eimeren	2 h	Bow - Aucissa openwork variant	Roman	5480
HS Elst	EM-533	Bow - Aucissa openwork variant	Roman	103346

Nijmegen worksheet - part 2 bulk elements

XRF No.	**Cu**	**Sn**	**Pb**	**Zn**	**Ag**	**Fe**
98097	76.32	19.47	1.41	0.19	0.09	1.75
98110	77.77	20.78	0.09	0.08	0.07	0.81
98113	56.95	28.05	9.32	0.41	0.26	3.17
98116	72.61	23.65	0.40	0.09	0.09	2.60
5511	62.05	32.82	0.23	0.16	0.17	1.53
5514	75.46	22.01	0.20	0.27	0.08	1.57
5582	77.84	18.76	0.91	0.30	0.12	1.36
102850	65.80	30.96	1.09	0.16	0.13	1.34
102851	58.55	35.21	0.78	0.10	0.10	4.72
102855	57.41	29.33	0.69	0.15	0.08	10.81
102856	71.79	25.27	0.62	0.61	0.11	1.02
102857	65.14	30.24	0.35	0.13	0.21	3.28
102860	68.30	27.02	0.66	0.17	0.25	2.80
102861	66.65	31.20	0.20	0.12	0.11	1.26
102862	63.84	31.33	0.44	0.22	0.17	3.22
102863	76.55	21.79	0.26	0.26	0.11	0.57
102864	46.64	39.98	1.04	0.50	0.16	10.03
102866	58.29	30.87	0.58	0.35	0.12	8.86
102867	76.03	22.30	0.23	0.17	0.12	0.58
102870	59.33	36.98	0.53	0.48	0.09	1.85
102875	74.35	22.49	0.75	0.14	0.16	1.54
102876	62.34	31.93	0.64	0.12	0.29	3.66
102877	62.10	31.88	0.53	0.12	0.11	4.38
102881	77.29	18.82	0.69	1.74	0.11	0.75
102886	57.71	33.07	0.40	0.83	0.13	6.83
102890	78.28	20.07	0.34	0.19	0.08	0.71
102892	66.61	30.67	0.57	0.25	0.11	1.38
102894	69.99	27.23	0.36	0.18	0.24	1.40

102895	55.15	34.04	0.68	0.17	0.12	8.80
102897	74.06	24.51	0.18	0.15	0.08	0.73
103199	76.50	21.07	0.17	0.09	<0,04	1.79
103201	70.95	25.71	0.56	0.08	0.25	1.41
103205	75.53	19.47	0.43	0.21	0.11	3.59
103211	59.59	37.92	0.46	0.13	0.15	1.17
103216	71.16	24.57	0.32	0.18	<0,05	3.27
103219	58.98	30.55	4.39	0.86	0.08	4.10
103222	76.98	16.97	0.22	0.18	0.08	4.55
103261	77.16	17.34	0.96	1.83	0.07	2.12
103267	78.88	1.10	2.67	11.56	0.07	4.90
103294	82.06	16.59	0.21	0.34	<0,05	0.42
103295	50.47	17.62	25.73	0.54	1.33	3.47
103303	76.71	21.35	0.06	<0,08	0.14	0.96
103322	60.81	34.40	0.88	0.17	0.23	2.76
103351	78.39	20.07	0.27	<0,07	0.08	0.37
98005	78.85	19.13	0.66	0.09	0.16	0.55
98019	84.34	14.67	0.14	0.07	0.08	0.46
98031	84.90	14.55	0.13	<0,09	<0,04	0.18
98036	75.38	20.83	0.89	0.21	0.10	2.17
98046	80.75	18.14	0.26	0.30	0.08	0.13
98050	66.30	28.26	0.27	0.27	0.09	3.87
98056	72.59	25.28	0.33	0.10	0.20	1.20
98060	77.37	10.68	1.16	0.18	0.07	10.18
98064	84.41	14.01	0.09	<0,06	0.16	1.04
98067	37.03	49.43	0.73	0.65	0.30	10.16
98068	60.78	32.10	0.74	0.48	0.11	4.87
98070	77.77	16.87	0.07	0.24	0.09	3.99
98078	36.21	41.58	1.59	3.72	0.18	14.95
98084	81.64	16.72	0.37	0.25	0.07	0.66
98090	79.48	18.49	0.34	0.15	0.12	1.07
98091	38.72	28.20	2.68	5.50	0.15	21.04
98105	48.64	37.87	1.51	5.57	0.43	4.63
98106	82.17	17.06	0.23	0.10	0.11	0.15
98111	71.75	23.91	1.61	1.53	0.10	0.62
98122	86.02	12.90	0.40	0.27	<0,03	0.22
98142	72.77	23.51	0.37	0.27	0.32	1.86
98153	74.43	18.72	0.70	0.58	0.27	4.52
98157	87.71	10.87	0.25	0.74	0.06	0.22
98169	87.08	9.76	0.42	1.92	0.10	0.39
98170	82.59	15.95	0.10	0.14	0.07	0.60
98171	61.24	34.24	0.82	0.42	0.20	1.46
98172	77.57	18.42	0.49	0.88	0.14	1.93
98174	67.63	20.40	0.25	0.40	0.16	9.98
98175	68.85	24.45	1.41	0.39	0.24	3.22
98181	77.07	19.63	0.51	0.32	0.36	1.21

5367	42.24	29.36	0.74	4.04	0.14	22.01
5394	41.42	11.05	38.53	3.79	0.11	4.31
5401	74.77	20.67	0.54	1.85	0.09	1.63
5404	72.10	22.09	2.31	0.85	0.22	1.16
5415	64.03	29.51	0.39	0.50	<0,1	4.49
5420	82.05	16.97	0.16	0.12	0.06	0.41
5463	56.42	38.42	0.33	0.18	0.23	3.44
5472	72.70	19.45	1.46	0.53	0.19	3.74
5474	81.35	16.61	0.12	<0,07	0.09	1.39
5476	58.31	33.86	3.33	0.61	0.12	3.03
5493	80.49	2.43	0.80	14.29	0.06	1.54
5518	79.40	18.30	0.55	0.66	0.07	0.58
5520	68.65	27.30	0.09	0.10	0.10	3.06
5524	62.59	14.84	2.16	0.33	<0,10	17.13
5527	65.75	20.88	0.88	0.83	0.12	9.44
5528	66.29	31.04	0.55	0.12	0.14	1.20
5537	58.72	23.27	2.29	5.71	0.14	8.39
5538	67.56	24.39	1.73	2.70	0.12	2.39
5546	64.44	26.39	1.15	3.27	0.08	3.73
5554	75.82	18.32	0.42	0.13	0.10	4.11
5558	51.36	40.23	1.88	1.15	0.12	4.28
5575	66.33	6.43	12.03	8.62	0.11	5.64
5576	72.03	19.79	0.70	0.43	0.15	5.00
5580	71.40	23.15	1.79	0.30	0.08	2.55
5586	82.37	16.36	0.16	0.19	0.17	0.39
5587	78.64	20.11	0.45	0.26	<0,03	0.33
5588	83.76	15.27	0.12	0.14	0.14	0.30
5593	66.41	4.32	5.52	8.64	0.11	12.52
5598	87.09	11.85	0.35	0.10	0.07	0.29
5599	84.57	14.12	0.38	0.38	0.08	0.22
5605	80.88	17.06	0.39	0.68	0.08	0.48
5607	43.29	43.91	0.46	0.22	0.13	10.18
5608	76.09	16.56	3.92	1.09	0.11	1.59
98058	67.31	25.37	2.14	1.21	0.17	2.67
98104	47.83	29.32	8.79	0.47	0.23	11.93
98109	85.61	0.52	1.21	11.11	0.08	1.21
5407	51.86	35.34	4.38	0.62	0.82	5.51
5414	79.54	18.77	0.20	0.28	0.08	0.65
5507	70.00	25.91	0.77	0.66	0.11	1.72
5519	50.73	39.34	1.15	0.50	0.23	6.53
5609	70.02	24.33	1.00	1.83	0.07	2.10
102901	56.47	36.77	0.15	0.17	0.18	5.35
102874	54.75	35.62	0.93	0.21	0.09	6.58
103350	63.12	31.83	0.83	0.60	0.11	2.68
103272	69.22	5.67	3.68	11.93	0.12	7.81
98053	85.88	2.04	1.64	7.77	0.11	2.09

98055	84.82	1.56	0.50	11.22	0.09	1.43
98069	86.43	0.49	1.40	7.06	0.12	3.83
98156	87.22	0.51	1.74	8.11	0.12	2.10
5470	85.36	0.06	0.59	12.63	<0,03	0.96
5496	88.92	0.18	0.55	8.56	<0,05	1.21
5525	68.99	1.52	4.57	6.59	0.09	16.01
5548	78.23	1.32	2.05	11.39	<0,03	6.40
5560	84.82	0.21	0.43	13.87	<0,03	0.54
102865	84.86	0.27	0.62	13.64	<0,03	0.43
103258	87.35	0.09	0.44	10.88	<0,02	1.05
98004	84.57	1.15	1.50	9.32	<0,03	2.71
98006	84.65	2.12	0.59	9.61	0.07	2.31
98021	83.38	0.43	0.35	11.54	<0,02	4.03
98080	88.00	0.20	1.20	8.88	0.07	1.35
98096	86.94	0.16	0.64	10.67	<0,02	1.38
98098	74.84	8.81	0.66	13.23	0.07	1.88
98119	86.18	2.31	0.46	10.51	<0,02	0.31
98132	82.30	1.12	0.62	12.32	0.09	2.90
98155	85.15	1.51	0.28	7.23	0.17	5.39
98182	84.92	1.37	2.35	6.44	0.13	4.38
5382	78.18	0.22	0.66	8.88	<0,03	10.51
5395	83.84	0.07	0.23	13.10	0.07	2.09
5397	84.23	0.08	0.77	12.20	<0,03	2.32
5421	86.18	0.35	0.27	12.29	<0,02	0.74
5424	83.38	1.15	0.36	14.32	0.11	0.34
5442	87.30	0.02	0.08	12.37	<0,02	0.09
5443	84.96	1.27	1.29	9.94	0.07	2.24
5447	81.08	0.43	1.77	9.97	<0,05	5.95
5461	86.26	1.50	0.24	10.35	<0,03	1.30
5471	75.88	10.85	1.38	4.96	0.06	6.31
5473	85.33	0.76	0.68	9.96	0.07	2.55
5487	71.07	4.95	3.16	4.23	0.17	15.70
5544	84.79	0.20	0.87	13.11	<0,03	0.80
5553	87.89	1.79	0.37	5.75	0.08	3.25
5578	82.34	2.62	0.98	9.19	0.12	4.04
5602	77.07	1.81	0.76	7.17	<0,05	10.39
5606	86.00	0.25	0.26	12.72	<0,02	0.58
103197	71.68	6.73	2.16	6.36	0.16	10.94
103202	88.15	0.05	0.25	10.38	0.08	0.70
103360	88.98	0.41	0.27	9.70	0.24	0.25
103343	86.28	1.15	0.88	6.91	<0,09	3.67
103292	88.27	0.18	0.38	10.18	0.07	0.65
103280	78.24	0.57	1.71	9.53	0.08	8.42
103260	90.74	0.04	0.45	7.02	0.07	1.36
103259	59.79	9.91	3.00	13.60	0.16	11.03
103221	86.95	1.02	0.36	10.82	0.06	0.55

103207	83.68	1.29	2.04	8.94	0.10	2.75
103341	83.20	1.17	2.99	8.19	<0,02	3.56
5501	77.53	0.55	0.97	18.82	<0,02	1.91
5426	83.29	1.88	3.87	7.15	0.12	3.04
98194	71.41	1.46	0.56	18.80	0.21	6.89
98144	94.47	0.13	0.64	3.27	0.14	1.11
98054	80.19	2.12	2.24	11.48	<0,03	3.55
98047	89.80	0.50	0.43	7.98	0.20	0.84
98079	46.49	18.45	25.93	3.60	0.08	4.58
98139	84.93	0.58	0.32	11.96	0.10	1.70
5455	89.95	0.05	0.60	8.05	0.23	0.77
5503	85.18	0.13	0.61	12.82	0.06	0.93
103320	83.78	0.18	0.64	13.51	0.12	1.32
103319	88.45	0.10	0.55	9.36	<0,03	1.24
103316	84.36	1.34	1.13	6.07	<0,03	6.63
103282	72.15	1.86	3.68	8.73	0.36	12.15
103269	89.63	0.59	1.17	7.14	0.07	0.98
103268	83.32	4.43	0.19	7.97	0.10	2.81
5396	83.86	1.73	1.37	8.76	0.21	3.42
5480	42.53	36.98	1.11	0.53	0.13	17.81
103346	73.52	2.42	3.41	12.35	0.07	7.34

Nijmegen worksheet - part 3 error

XRF No.	Cu error	Sn error	Pb error	Zn error	Ag error	Fe error
98097	0.13	0.10	0.06	0.03	0.02	0.05
98110	0.12	0.11	0.02	0.03	0.02	0.04
98113	0.18	0.14	0.13	0.03	0.02	0.09
98116	0.12	0.10	0.03	0.02	0.02	0.06
5511	0.16	0.15	0.03	0.03	0.02	0.07
5514	0.11	0.09	0.02	0.03	0.02	0.05
5582	0.13	0.10	0.05	0.03	0.02	0.05
102850	0.20	0.19	0.07	0.04	0.03	0.08
102851	0.21	0.21	0.06	0.04	0.03	0.13
102855	0.20	0.16	0.05	0.04	0.03	0.16
102856	0.19	0.16	0.05	0.05	0.03	0.07
102857	0.16	0.15	0.03	0.03	0.03	0.09
102860	0.20	0.17	0.06	0.04	0.03	0.10
102861	0.20	0.18	0.03	0.04	0.03	0.08
102862	0.16	0.15	0.04	0.03	0.02	0.09
102863	0.17	0.14	0.04	0.04	0.03	0.05
102864	0.31	0.31	0.08	0.07	0.04	0.26
102866	0.17	0.15	0.04	0.04	0.02	0.14
102867	0.16	0.13	0.03	0.04	0.03	0.05
102870	0.20	0.19	0.05	0.05	0.03	0.09
102875	0.16	0.13	0.05	0.03	0.03	0.06
102876	0.22	0.20	0.06	0.04	0.04	0.13
102877	0.20	0.19	0.05	0.04	0.03	0.13
102881	0.21	0.16	0.07	0.08	0.03	0.06
102886	0.22	0.20	0.04	0.06	0.03	0.16
102890	0.14	0.11	0.03	0.03	0.02	0.04
102892	0.24	0.21	0.06	0.05	0.03	0.09
102894	0.22	0.19	0.05	0.05	0.04	0.08
102895	0.22	0.20	0.05	0.04	0.03	0.17
102897	0.16	0.13	0.03	0.03	0.02	0.05
103199	0.13	0.11	0.02	0.03	0.04	0.06
103201	0.17	0.15	0.05	0.03	0.03	0.07
103205	0.14	0.11	0.04	0.03	0.02	0.08
103211	0.20	0.20	0.04	0.04	0.03	0.08
103216	0.16	0.14	0.04	0.04	0.05	0.09
103219	0.19	0.17	0.11	0.05	0.03	0.11
103222	0.13	0.10	0.03	0.03	0.02	0.08
103261	0.19	0.12	0.06	0.07	0.02	0.07
103267	0.22	0.03	0.10	0.13	0.02	0.08
103294	0.16	0.12	0.03	0.04	0.05	0.04
103295	0.18	0.10	0.16	0.03	0.03	0.09
103303	0.18	0.15	0.02	0.08	0.03	0.06

103322	0.21	0.20	0.06	0.04	0.03	0.11
103351	0.15	0.12	0.03	0.07	0.02	0.04
98005	0.12	0.09	0.04	0.03	0.02	0.03
98019	0.11	0.08	0.02	0.03	0.02	0.03
98031	0.12	0.09	0.02	0.09	0.04	0.02
98036	0.13	0.11	0.05	0.03	0.02	0.06
98046	0.11	0.09	0.03	0.03	0.02	0.02
98050	0.15	0.13	0.03	0.03	0.02	0.09
98056	0.17	0.15	0.04	0.04	0.03	0.06
98060	0.23	0.10	0.08	0.05	0.03	0.15
98064	0.11	0.08	0.02	0.06	0.02	0.04
98067	0.22	0.26	0.05	0.05	0.03	0.19
98068	0.19	0.17	0.05	0.04	0.03	0.12
98070	0.13	0.09	0.02	0.03	0.02	0.08
98078	0.21	0.21	0.06	0.09	0.03	0.19
98084	0.11	0.09	0.03	0.03	0.02	0.03
98090	0.13	0.10	0.03	0.03	0.02	0.05
98091	0.23	0.16	0.08	0.11	0.03	0.20
98105	0.22	0.19	0.07	0.10	0.03	0.12
98106	0.11	0.08	0.02	0.03	0.02	0.02
98111	0.16	0.13	0.07	0.05	0.02	0.04
98122	0.10	0.07	0.03	0.03	0.03	0.02
98142	0.11	0.09	0.02	0.02	0.02	0.04
98153	0.10	0.07	0.02	0.02	0.02	0.04
98157	0.08	0.05	0.02	0.02	0.02	0.01
98169	0.08	0.05	0.02	0.03	0.02	0.01
98170	0.08	0.05	0.01	0.02	0.02	0.02
98171	0.11	0.11	0.03	0.02	0.02	0.04
98172	0.10	0.07	0.02	0.03	0.02	0.03
98174	0.11	0.08	0.02	0.02	0.02	0.07
98175	0.10	0.08	0.03	0.02	0.02	0.04
98181	0.10	0.08	0.02	0.02	0.02	0.03
5367	0.28	0.20	0.06	0.12	0.03	0.24
5394	0.18	0.09	0.18	0.07	0.02	0.09
5401	0.17	0.13	0.05	0.06	0.02	0.07
5404	0.37	0.25	0.17	0.09	0.05	0.11
5415	0.36	0.31	0.07	0.08	0.10	0.21
5420	0.11	0.09	0.02	0.03	0.02	0.03
5463	0.20	0.20	0.04	0.04	0.03	0.12
5472	0.65	0.39	0.23	0.14	0.09	0.29
5474	0.14	0.11	0.02	0.07	0.02	0.06
5476	0.24	0.21	0.12	0.05	0.03	0.12
5493	0.20	0.05	0.06	0.14	0.02	0.05
5518	0.16	0.12	0.05	0.05	0.02	0.04
5520	0.15	0.13	0.02	0.03	0.02	0.08
5524	0.38	0.18	0.14	0.07	0.10	0.28

5527	0.34	0.22	0.10	0.09	0.05	0.23
5528	0.15	0.14	0.04	0.03	0.02	0.06
5537	0.29	0.19	0.11	0.14	0.03	0.17
5538	0.30	0.20	0.11	0.11	0.04	0.12
5546	0.23	0.17	0.07	0.09	0.03	0.12
5554	0.19	0.14	0.05	0.04	0.03	0.11
5558	0.19	0.19	0.07	0.05	0.03	0.12
5575	0.21	0.07	0.15	0.11	0.02	0.09
5576	0.14	0.10	0.04	0.03	0.02	0.09
5580	0.15	0.12	0.07	0.03	0.02	0.07
5586	0.13	0.10	0.02	0.03	0.02	0.03
5587	0.13	0.10	0.03	0.03	0.03	0.03
5588	0.13	0.10	0.02	0.03	0.02	0.03
5593	0.31	0.07	0.15	0.15	0.03	0.15
5598	0.11	0.08	0.03	0.03	0.02	0.02
5599	0.11	0.08	0.03	0.03	0.02	0.02
5605	0.12	0.09	0.03	0.04	0.02	0.03
5607	0.21	0.23	0.04	0.04	0.03	0.18
5608	0.17	0.10	0.10	0.05	0.02	0.06
98058	0.18	0.14	0.08	0.05	0.02	0.08
98104	0.19	0.15	0.12	0.04	0.02	0.15
98109	0.13	0.02	0.06	0.09	0.01	0.03
5407	0.21	0.19	0.11	0.05	0.04	0.14
5414	0.16	0.13	0.03	0.04	0.03	0.05
5507	0.14	0.12	0.04	0.04	0.02	0.06
5519	0.23	0.23	0.07	0.05	0.03	0.17
5609	0.15	0.12	0.05	0.05	0.02	0.07
102901	0.20	0.20	0.03	0.04	0.03	0.14
102874	0.19	0.18	0.05	0.04	0.03	0.14
103350	0.17	0.16	0.05	0.04	0.02	0.09
103272	0.31	0.09	0.14	0.18	0.03	0.14
98053	0.17	0.04	0.08	0.10	0.02	0.05
98055	0.14	0.03	0.04	0.10	0.01	0.04
98069	0.16	0.02	0.06	0.08	0.02	0.06
98156	0.11	0.01	0.05	0.05	0.01	0.03
5470	0.17	0.01	0.05	0.12	0.03	0.03
5496	0.13	0.01	0.04	0.09	0.05	0.03
5525	0.33	0.05	0.15	0.14	0.03	0.19
5548	0.19	0.03	0.07	0.11	0.03	0.08
5560	0.18	0.02	0.04	0.13	0.03	0.03
102865	0.18	0.02	0.05	0.13	0.03	0.03
103258	0.13	0.01	0.03	0.09	0.02	0.03
98004	0.16	0.03	0.07	0.09	0.03	0.05
98006	0.13	0.03	0.04	0.08	0.01	0.04
98021	0.12	0.01	0.03	0.08	0.02	0.05
98080	0.11	0.01	0.05	0.07	0.01	0.03

98096	0.11	0.01	0.04	0.08	0.02	0.03
98098	0.15	0.06	0.04	0.10	0.02	0.04
98119	0.12	0.03	0.03	0.08	0.02	0.02
98132	0.17	0.03	0.05	0.11	0.02	0.06
98155	0.07	0.02	0.02	0.04	0.01	0.03
98182	0.13	0.02	0.04	0.04	0.01	0.04
5382	0.18	0.01	0.04	0.09	0.03	0.09
5395	0.14	0.01	0.03	0.10	0.01	0.04
5397	0.16	0.01	0.05	0.10	0.03	0.04
5421	0.12	0.01	0.03	0.09	0.02	0.02
5424	0.11	0.02	0.03	0.09	0.01	0.02
5442	0.10	0.01	0.01	0.08	0.02	0.01
5443	0.13	0.02	0.05	0.08	0.01	0.04
5447	0.18	0.02	0.07	0.10	0.05	0.07
5461	0.13	0.03	0.02	0.09	0.03	0.03
5471	0.23	0.10	0.08	0.11	0.03	0.12
5473	0.18	0.02	0.05	0.11	0.02	0.05
5487	0.17	0.04	0.08	0.07	0.02	0.11
5544	0.15	0.01	0.05	0.11	0.03	0.03
5553	0.13	0.03	0.03	0.07	0.02	0.05
5578	0.14	0.03	0.05	0.08	0.01	0.05
5602	0.21	0.04	0.05	0.10	0.05	0.11
5606	0.11	0.01	0.02	0.09	0.02	0.02
103197	0.22	0.07	0.09	0.11	0.03	0.13
103202	0.11	0.01	0.02	0.08	0.01	0.02
103360	0.10	0.01	0.02	0.07	0.01	0.01
103343	0.29	0.04	0.09	0.14	0.09	0.10
103292	0.11	0.01	0.03	0.08	0.01	0.02
103280	0.16	0.02	0.06	0.09	0.01	0.08
103260	0.11	0.01	0.03	0.07	0.01	0.03
103259	0.21	0.07	0.08	0.12	0.02	0.11
103221	0.11	0.02	0.03	0.09	0.01	0.02
103207	0.16	0.03	0.07	0.09	0.02	0.05
103341	0.14	0.02	0.07	0.07	0.02	0.05
5501	0.14	0.02	0.04	0.10	0.02	0.03
5426	0.16	0.03	0.09	0.08	0.02	0.05
98194	0.13	0.03	0.03	0.09	0.02	0.05
98144	0.07	0.01	0.02	0.03	0.01	0.02
98054	0.16	0.03	0.07	0.10	0.03	0.06
98047	0.11	0.02	0.03	0.07	0.01	0.02
98079	0.19	0.12	0.18	0.07	0.02	0.10
98139	0.12	0.02	0.03	0.09	0.01	0.03
5455	0.13	0.01	0.04	0.08	0.02	0.03
5503	0.13	0.01	0.04	0.09	0.01	0.03
103320	0.12	0.01	0.04	0.09	0.01	0.03
103319	0.13	0.01	0.04	0.08	0.03	0.03

103316	0.14	0.02	0.05	0.07	0.03	0.07
103282	0.18	0.03	0.09	0.09	0.02	0.10
103269	0.11	0.02	0.05	0.07	0.01	0.03
103268	0.14	0.05	0.02	0.09	0.02	0.05
5396	0.13	0.03	0.05	0.08	0.01	0.05
5480	0.24	0.22	0.06	0.05	0.03	0.22
103346	0.19	0.03	0.09	0.11	0.02	0.08

Corrosion Experiment Worksheet part 1 typological data

Collection	Find ID	Description	XRF No.
HS Elst	EM-018b	Bow - Almgren 15 - Corr.	103140
HS Elst	EM-018b	Bow - Almgren 15 - Clean	103142
HS Elst	EM-018a	Bow - Almgren 20 - Corr.	103143
HS Elst	EM-018a	Bow - Almgren 20 - Clean	103144
HS Elst	EM-007	Bow - Almgren 20 - Corr.	103145
HS Elst	EM-007	Bow - Almgren 20 - Clean	103146
HS Elst	EM-016	Bow - knee-brooch Böhme 19, foot - Corr.	103147
HS Elst	EM-016	Bow - knee-brooch Böhme 19, foot - Clean	103148
HS Elst	EM-095	Bow - Corr.	103149
HS Elst	EM-095	Bow - Clean	103150
HS Elst	EM-142	Bow - Corr.	103151
HS Elst	EM-142	Bow - Clean	103152
HS Elst	EM-492	Bow - Almgren 20 - Corr.	103153
HS Elst	EM-492	Bow - Almgren 20 - Clean	103154
HS Elst	EM-140	Bow - Corr.	103155
HS Elst	EM-140	Bow - Clean	103156
HS Elst	EM-540	Bow - Almgren 20 - Corr.	103159
HS Elst	EM-540	Bow - Almgren 20 - Clean	103160
HS Elst	EM-902	Bow - Corr.	103163
HS Elst	EM-902	Bow - Clean	103165
HS Elst	EM-552	Bow - Almgren 15 - Corr.	103166
HS Elst	EM-552	Bow - Almgren 15 - Clean	103167
HS Elst	EM-655	Bow - Van Buchem 24 - Corr	103168
HS Elst	EM-655	Bow - Van Buchem 24 - Clean	103170
HS Elst	EM-597	Bow - Almgren 15 - Corr.	103171
HS Elst	EM-597	Bow - Almgren 15 - Clean	103172
HS Oosterhout	OA-145	Bow - Eye series, foot, frag - Corr	103173
HS Oosterhout	OA-145	Bow - Eye series, foot, frag - Clean	103174

Corrosion Experiment Worksheet part 2 bulk elements

XRF No.	Cu	Sn	Pb	Zn	Ag	Fe
103140	41.89	44.75	1.79	0.45	0.30	9.23
103142	87.66	10.91	0.40	<0,13	0.12	0.39
103143	78.81	5.78	1.69	8.74	0.12	4.12
103144	79.01	1.35	0.27	18.97	<0,04	0.23
103145	85.95	0.27	0.55	11.87	<0,03	1.10
103146	80.74	0.17	0.35	17.99	<0,04	0.64
103147	55.22	36.50	1.33	0.51	0.11	5.63
103148	85.90	12.98	0.29	0.31	<0,05	0.27
103149	43.77	27.06	0.12	0.20	0.13	25.77
103150	85.43	13.65	0.05	<0,07	0.10	0.42
103151	35.26	49.81	5.67	0.57	0.17	7.52
103152	83.36	13.44	2.07	0.66	0.07	0.20
103153	85.02	0.53	0.80	11.16	0.07	1.85
103154	79.29	0.29	0.36	19.54	<0,02	0.43
103155	21.15	59.54	0.30	0.17	0.09	17.32
103156	81.37	17.77	0.05	<0,09	<0,05	0.48
103159	81.75	1.28	0.50	9.62	0.07	5.55
103160	80.77	0.57	0.11	17.92	<0,03	0.39
103163	69.25	17.80	1.26	4.81	0.15	6.02
103165	87.27	6.61	0.36	4.77	<0,10	0.61
103166	78.57	20.10	0.45	0.18	0.07	0.31
103167	86.04	13.36	0.25	0.08	<0,05	0.11
103168	63.59	24.88	0.72	5.20	0.13	4.69
103170	85.75	7.61	0.17	6.06	<0,04	0.29
103171	71.87	25.44	0.56	0.56	0.09	1.02
103172	83.78	14.84	0.23	0.45	0.08	0.32
103173	79.65	5.86	1.81	8.07	0.08	3.68
103174	77.99	1.34	0.19	20.15	<0,05	0.19

Corrosion Experiment Worksheet part 3 error

XRF No.	Cu error	Sn error	Pb error	Zn error	Ag error	Fe error
103140	0.27	0.29	0.09	0.05	0.04	0.23
103142	0.30	0.17	0.08	0.13	0.04	0.06
103143	0.23	0.08	0.10	0.14	0.03	0.09
103144	0.25	0.04	0.04	0.18	0.04	0.02
103145	0.16	0.02	0.05	0.11	0.03	0.04
103146	0.24	0.02	0.05	0.17	0.04	0.04
103147	0.24	0.23	0.08	0.05	0.03	0.16
103148	0.18	0.12	0.04	0.05	0.05	0.03
103149	0.28	0.20	0.03	0.05	0.04	0.27
103150	0.14	0.11	0.02	0.07	0.02	0.04
103151	0.22	0.26	0.12	0.04	0.03	0.18
103152	0.17	0.11	0.10	0.05	0.02	0.03
103153	0.13	0.02	0.04	0.09	0.01	0.04
103154	0.16	0.01	0.03	0.12	0.02	0.02
103155	0.26	0.37	0.04	0.04	0.04	0.31
103156	0.19	0.15	0.02	0.09	0.05	0.05
103159	0.33	0.05	0.07	0.17	0.03	0.12
103160	0.19	0.02	0.02	0.14	0.03	0.02
103163	0.22	0.13	0.07	0.10	0.03	0.12
103165	0.50	0.17	0.10	0.20	0.10	0.08
103166	0.14	0.12	0.04	0.04	0.02	0.03
103167	0.15	0.11	0.04	0.04	0.05	0.02
103168	0.21	0.16	0.06	0.11	0.03	0.12
103170	0.16	0.07	0.03	0.09	0.04	0.03
103171	0.23	0.19	0.06	0.06	0.03	0.08
103172	0.25	0.17	0.05	0.07	0.04	0.05